Theory of the Stereological Analysis of Spheroid Size Distribution – Validation of the Equations

D. Gurgul, A. Burbelko *, T. Wiktor
AGH University of Science and Technology,
23 Reymonta Str., 30-059 Krakow, Poland
* Corresponding author. E-mail address: abur@agh.edu.pl

Abstract

The paper presents validation tests for method which is used for the evaluation of the statistical distribution parameters for 3D particles' diameters. The tested method, as source data, uses chord sets which are registered from a random cutting plane placed inside a sample space. In the sample space, there were individually generated three sets containing 3D virtual spheres. Each set had different Cumulative Distribution Function (CDF_3) of the sphere diameters, namely: constant radius, normal distribution and bimodal distribution as a superposition of two normal distributions. It has been shown that having only a chord set it is possible, by using the tested method, to calculate the mean value of the outer sphere areas. For the sets of data, a chord method generates quite large errors for around 10% of the smallest nodules in the analysed population. With the increase of the nodule radii, the estimation errors decrease.
The tested method may be applied to foundry issues e.g. for the estimation of gas pore sizes in castings or for the estimation of nodule graphite sizes in ductile cast iron.

Keywords: Stereological analysis, Linear analysis, Nodule size distribution

1. Introduction

The problem of the mapping of an unknown probability distribution of the spherical particle sizes in a non-transparent substance is one of the classical stereological tasks. When the density of the analysed particles is very much different from the density of the matrix phase, it is possible, for this kind of the analysis, to use the X-ray micro-tomography method [1]. There is also a possibility to evaluate the statistical distribution of the 3D nodule size by using stereological methods which base on a statistical distribution of the diameters on 2D or base on a random chord length distribution obtained by linear analysis from random secants.

2. Model assumption

Let us assume that the fraction of the visible circular sections with radius $r_2 \leq t$ on a random plane section is given by the function $F_2(t)$ named Cumulative Distribution Function (CDF_2). Let us assume also that the fraction of the chords with the length $2 \cdot r_1 \leq 2 \cdot t$ placed inside the particles is given by the function $F_1(t)$ (designated as CDF_1).

The largest section radius, as well as the largest half-length of chord for a random round cross-section of particles are limited by the maximal radius R_{max} of the largest sphere.

Each $F_i(t)$ presented above has its Probability Density Function $f_i(t)$ (designated as PDF_i):

$$f_i(t) = \begin{cases} 0 & t < 0 \\ dF_i/dt & \text{for} \quad 0 \le t < R_{\max} \\ 0 & t \ge R_{\max} \end{cases} \tag{1}$$

where $i = 1$ for half-length of the chord, 2 for the radii of cross-section, and 3 for the radii of the nodules.

First known solution to the PDF_3 mapping based on the measured PDF_2 has been proposed by Wicksell [2]:

$$f_2(t) = \frac{t}{E[r_3]} \int_t^{R_{\max}} \frac{f_3(x)}{\sqrt{x^2 - t^2}} \, dx \tag{2}$$

were $R_{\max}$ is the radius of the biggest particle in the probe, $E[r_3]$ is the expected (mean) values of the nodule radius, x is the variable of integration.

When the empirical function $f_2(t)$ was estimated by quantitative metallography methods, equation (2) can be solved with respect to the integrand $f_3(x)$ by the implicit solution. In this task such a solution (named sometimes as inverse) according to [3] gives the unsatisfactory results. This is the reason why the numerical solutions of this task are used most often. The analysis of the planar section which bases on the direct Wickesell equation (2) has been used for the volume size distribution of the spheroidal particles by Scheil [4], Schwartz [5], Saltykov [6,7], Li at al. [8]. A similar solution to the mineralogy task has been presented in [9]. Unfortunately, small numerous errors of the empirically estimated function $f_2(t)$ result in the „*arbitrarily large perturbations of the solution*" [10,11]. In this context, Eq. (2) is usually used not for the designation of the PDF_3 form, but for the examination of matching the empirical function and one of the selected statistical distribution law, e.g. normal, log-normal, Weibull or uniform-sized [3,8,12].

Other stereological method for the calculation of the size distribution of spheres randomly distributed in 3D space was proposed by Cahn and Fullmann [13], Lord and Willis [14], and Spektor [15]. This method bases on the measurements of the PDF_1 of the corresponding chord-length distribution obtained through lineal analysis:

$$f_3(t) = \frac{N_1}{2\pi N_3} \left[\frac{f_1(t)}{t^2} - \frac{1}{t} \frac{d f_1(t)}{dt} \right] \tag{3}$$

where N_3 is the total number of the grains per unit volume, and N_1 is the total number of the chords per unit length of the measuring lines.

For the practical usage of the above equation Bockstiegel [16] has proposed dividing the interval of the measured chord length into segments l_j with the length that varies geometrically $l_i = \sqrt{2} l_{i-1}$. For this scale of the chord length

$$N_{3,i} - N_{3,i-1} = \frac{4}{\pi} \frac{3N_{1,i} - 2N_{1,i-1} - N_{1,i+1}}{l_i} \tag{4}$$

where $N_{3,i}$ is the number of the nodules and $N_{1,i}$ is the number of the chord with the diameter (length) that does not exceed l_i. The limitation of this solution is the low resolution for the large diameter of the particles which is a result of the logarithmic nature of the scale.

According to [17] the empirical CDF_3 for spherical particle radii should be estimated on the basis of the empirical estimation of PDF_1 of half-length chords t as follows:

$$F_3(t) = 1 - \frac{\overline{S}}{8\pi t} f_1(t) \tag{5}$$

where $\overline{S}$ is the mean external surface of nodules in the probe.

3. Data preparation

In order to test the precision of the proposed method, for the evaluation of the CDF_3 form on the basis of the PDF_1 given by eq. (5), three virtual sets of nodules were generated. The nodules are randomly distributed in the volume of size equal to $8 \cdot a \cdot b \cdot R_{\max}$ (Fig. 1). These particles are cut by a base plane on which a set of parallel secants are placed. The 2D section diameters and length of the chords, made by the secants, are measured and collected. The virtual probe space, in which the particles were generated, fulfils the following conditions:

- The mean grain density in the specimen volume is equal to N_3 (number grains per unit volume).
- The spatial distribution of the grain centres is defined by the Poisson statistical distribution.
- The probability of intersection between the particles is negligible (or for the intersected particles it is possible to indicate and measure the diameter of every nodule).

Each linear dimension which will be mentioned in the later part of the paper, is expressed by convention in a unit length (ul). Similarly, all measured and calculated areas are also expressed by convention in a surface unit (1 us = 1 ul^2).

The virtual sets of nodules were generated as follows: In the first stage the set of radii r_{3i} (for $i = 1 \ldots N$) is generated by using a pseudo-random number generator for three types of CDF_3 which will be described in the next section. In the next step among all generated particles, it is necessary to find the radius $R_{\max}$ of the greatest nodule. The last step is to generate, by using the uniform pseudo-random number generator, the centre coordinates (x_i, y_i, z_i) for all nodules. The coordinates are distributed in the following range:

$$\begin{aligned} x &\in (-a + R_{\max}; \, a - R_{\max}) \\ y &\in (-b + R_{\max}; \, b - R_{\max}) \\ z &\in (-R_{\max}; \, R_{\max}) \end{aligned} \tag{6}$$

Having fulfilled the above conditions, the results of the virtual stereological measurements are registered from the rectangular test plane T shown in Fig. 1:
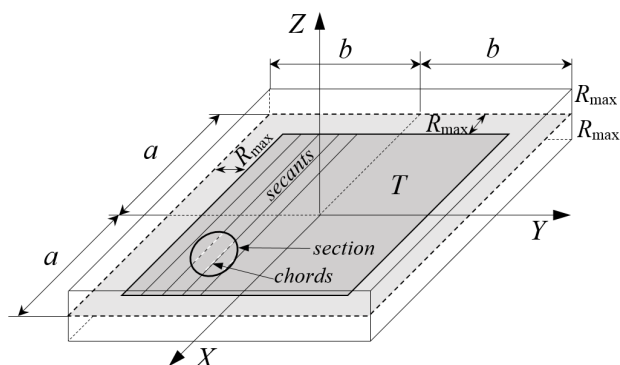
Fig. 1. The specimen volume in which the virtual nodules were generated. Legend: T – the cutting plane from which the chords are collected; R_{max} – the maximum radius of a generated nodule

The measuring plane T is parallel to XY axes and cut the Z axis in zero. All secants are parallel to the X axis and have the same distance between each other equal to k. The secants cut through the 2D section and form the chords (the fragments of the secant inside the nodules sections). Only these particles and sections are taken into account which the central points (x and y coordinates) lie on the T area (excluding the R_{max} margins). The aim of such an approach is to eliminate the bias error created by the overestimation of the nodules with small sizes.

Between the nodules and their sections, chords and central points, there are the following geometrical relations:

- for the nodule i with the radius r_{3i} its radius r_{2i} of the section is equal to:

$$r_{2i} = \sqrt{r_{3i}^2 - z_i^2} \tag{7}$$

- the relation between the radius of the nodule i and its length of the chord ($r_{i,j}$), the coordinates of the particle centre (y_i) and the coordinates of the measuring secant j ($y_{a,j}$) is as follows:

$$r_{3i}^2 = z_i^2 + r_{i,j}^2 + \left(y_i - y_{a,j}\right)^2 \tag{8}$$

Hence the half-length of the random chord j of the nodule i will be equal to:

$$r_{1,i,j} = \sqrt{r_{3i}^2 - z_i^2 - \left(y_i - y_{a,j}\right)^2} \tag{9}$$

4. Data analysis

In order to check the application of the equation (5) for the evaluation of the $F_3(t)$, three sets of data have been prepared. Each set has different PDF$_3$ of the nodules radii:

A. The set of nodules with a constant radius equal to $r_3 = 200$. The total Number of particles is $N = 1024$.

B. The normal distribution with the mean value $\bar{r}_3 = 120$, and the standard deviation $\sigma = 15$, $N = 2048$.

C. The bimodal distribution as the superposition of two normal distributions with the parameters $\bar{r}_{3,1} = 90$, $\sigma_1 = 10$, $N_1 = 2048$ and $\bar{r}_{3,2} = 150$, $\sigma_2 = 15$, $N_1 = 1024$.

In order to obtain the sets with the normal distribution, the inverse cumulative distribution function method was used. The data was generated by using the **vdRngGaussian** function from the MKL library [18]. Whereas for generating the nodules' central points, the **vRngUniform** function from this library was used.

The cumulative distribution functions and probability density functions for the analysed sets of the half-length chords are calculated by empirical equations:

$$F_1(t_i) = \frac{N_i}{N} \tag{10}$$

$$f_1(t_i) = \frac{N_i - N_{i-1}}{N(t_i - t_{i-1})} \tag{11}$$

where N_i is the chord numbers with a length no longer than $2t_i$. For the calculation the sets of r_1 were sorted in an ascending order. In the calculations the length of every five hundred chord or every thousandth was taking into account. The results for 1 out of 500 chords are presented in the fig. 2.

If in the sample there are no spherical particles with a radius less than R_{min}, then it is possible to estimate the value of the mean external surface of the nodules $\bar{S}$ on the basis of measurements obtained for interval ($0 < t < R_{min}$) by the following equation:

$$S_{est} = \frac{8\pi t}{f_1(t)} \tag{12}$$

By substituting the equation (11) into (12) we obtain:

$$S_{est} = 8\pi N t_i \frac{t_i - t_{i-1}}{N_i - N_{i-1}} \tag{13}$$

This means that for $t_i < R_{min}$ the estimation of the S_{est} may be obtained by equation (13) after the substitution of the data for any interval i of the chord length (provided that the measured data is free of noise). The results received by this equation are presented in fig 3. In the case of the **A** distribution for the whole interval of the measured chords, the calculated results are characterised by the mean value $S_{est\,A} = 502 \cdot 10^3$ us, with the standard deviation $\sigma_A = 34 \cdot 10^3$ us. The results for two first intervals are clearly bigger than the rest and were eliminated from the calculation. The precise value of the outer area for the sphere with the radius $r_3 = 200$ ul is equal to 502 655 us.
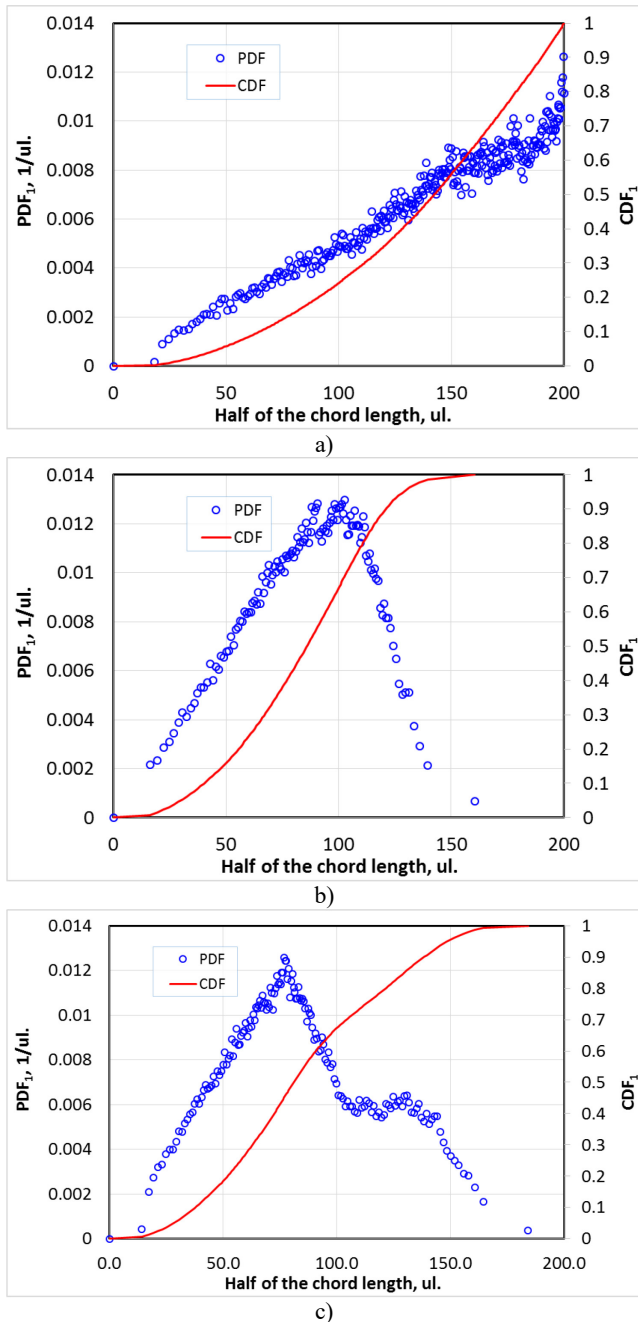
a)

b)

c)

Fig. 2. The shapes of the empirical cumulative distribution functions and probability density functions for the prepared sets of nodules: a) constant r_3 – A; b) normal – B; c) bimodal – C

In the case of **B** and **C** distributions, there are distinguishing horizontal intervals that indicate the absence (or negligible low number) of the nodules with a radius less than around 70-80 ul. The mean values of the S_{est} and the standard deviation for the radii which are less than 70 ul are following:

- for the **B** distribution: the mean value $S_{est\ B} = 181.9 \cdot 10^3$ us, the standard deviation $\sigma_B = 8.6 \cdot 10^3$ us,

- for the **C** distribution: the mean value $S_{est\ C} = 161.7 \cdot 10^3$ us, the standard deviation $\sigma_C = 7.3 \cdot 10^3$ us.

Similarly to the case of the **A** distribution, the results from the three first intervals (that give results clearly bigger than the rest) were eliminated from the calculation.
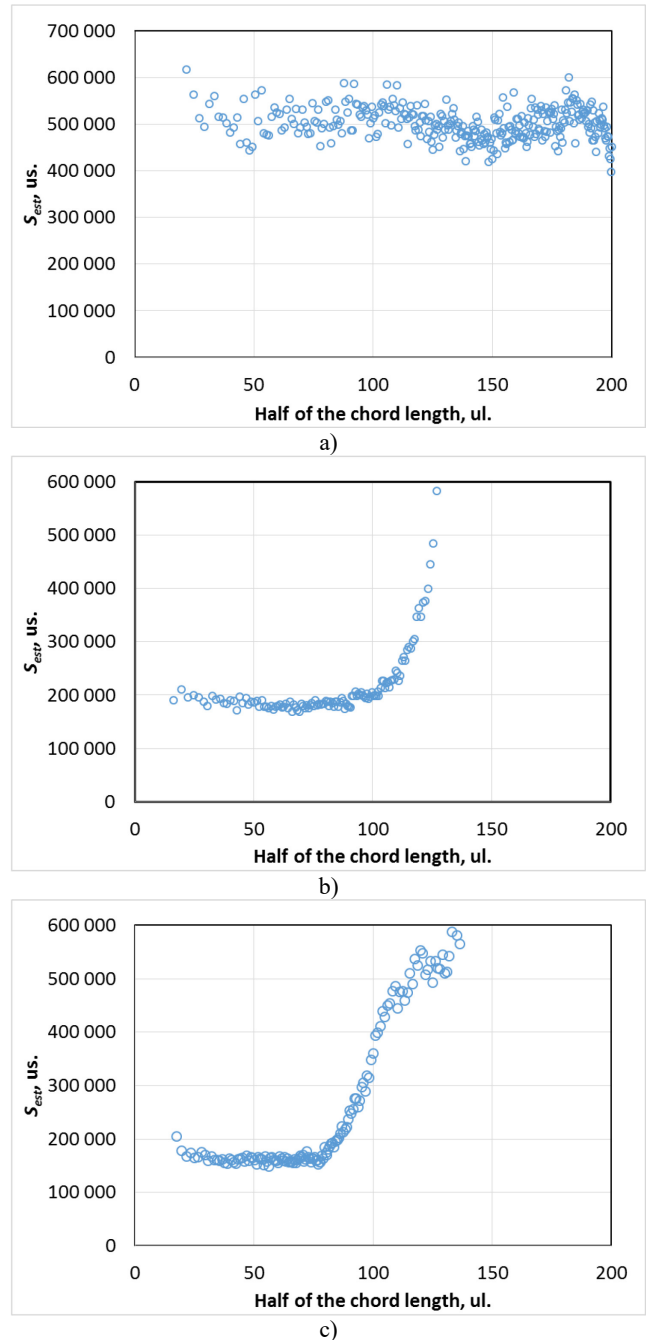

a)

b)

c)

Fig. 3. Cumulative distribution functions and probability density functions of the half-length of the chords for the nodular particle sets for the distributions: a) constant radius r_3 – **A**; b) normal **B**; c) bimodal **C**

For comparison, the precise values of the mean outer areas, which were calculated directly on the base of the source data, are equal to 182 406 us for the set **B** and 162 774 us for the set **C** respectively. As it follows from the above data, the results of the estimation obtained by the proposed method are similar to the real parameters of the analysed set of nodular particles.

The cumulative distribution functions of the nodular particles returned by the eq. (5) on the base of the source data for the sets **B** and **C** are presented in Fig. 4. The results of the direct calculation on the basis of the bench-mark data are presented by solid lines. The dependence obtained by the means of eq. (5) is indicated by the dots. As it follows from the pictures, the proposed method has a lower accuracy at the interval close to 10% of the smallest nodules of the analysed population. With the increase of the nodule radii, the accuracy of the CDF_3 mapping by the chords method increases and for the particles with big sizes, the accuracy of mapping is reasonable.
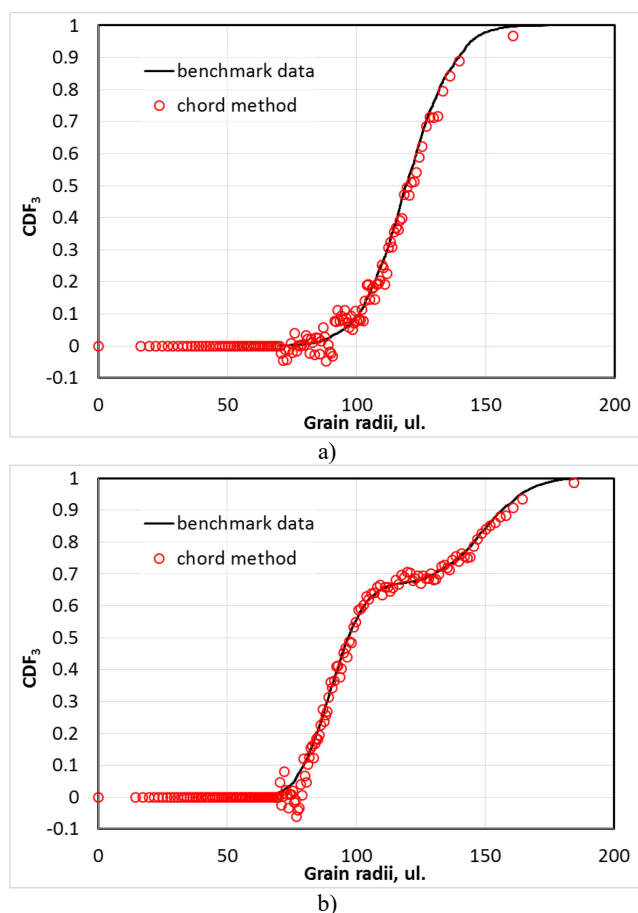

Fig. 4. Empirical cumulative distribution function of the nodular particles: direct calculation on the base of the source data (solid lines) and the results of the mapping by means of the chords method (dots): a) for normal distribution – set **B**; b) for bimodal distribution – set **C**

5. Conclusions

- The empirical CDF_3 of the nodular size particles can be estimated on the basis of the empirical measurement of PDF_1. For the estimation of CDF_3, it is necessary to use Eq (5) and the statistical distribution of random chord lengths received from experimental data.
- In the calculations, the results must be used from the interval, where the estimation of the mean value of the outer particle surface by means of the eq. (12) is constant.
- For the used sets of the source data, the proposed chord method has a lower accuracy at the interval close to 10% of the smallest nodules of the analysed population. With the increase of the nodule radii, the accuracy of the CDF_3 mapping by the chord method increases and for the particles with big sizes, the accuracy of mapping is reasonable.

Acknowledgment

References

[1] Yin, Y., Tu, Z., Zhou, J. at al. (2017). 3D Quantitative Analysis of Graphite Morphology in Ductile Cast Iron by X-ray Microtomography. *Metallurgical and Materials Transactions A*. 48(8), 3794-3803. DOI: 10.1007/s11661-017-4130-x.

[2] Wicksell, S.D. (1925). The Corpuscle Problem: A Mathematical Study of a Biometric Problem. *Biometrika*. 17(1/2), 84-99.

[3] Więcek, K., Skowronek, K. & Khatemi, B. (2005). Graphite particles size distribution in nodular cast iron. *Metallurgy and Foundry Engineering*. 31(2), 167-173.

[4] Sheil, E. (1935). Statistische Gefügeuntersuchungen. *I. Z. Metallk*. 27, 199-208.

[5] Schwartz, H.A. (1934). The Metallographie Determination of the Size Distribution of Temper Carbon Nodules. *Metals and Alloys*. 5, 139-140.

[6] Saltykov, S.A. (1952). *Stereometric Metallurgy*, Ind. Ed., Metallurgizdat, Moscow.

[7] Saltykov, S.A. (1967). The determination of the size distribution of particles in an opaque material from the measurement of the size distribution of their sections. *Stereology*. Berlin, Heidelberg, Springer, 163-173.

[8] Li, T., Shimasaki, S.-i., Taniguchi, Sh. & Narita, Sh. (2016). Reliability of Inclusion Statistisc in Steel Stereological Methods. *ISIJ International*. 56(9), 1625-1633.

[9] Kong, M., Bhattacharya, R.N., James, C. & Basu, A. (2005). A statistical approach to estimate the 3D size distribution of spheres from 2D size distributions. *GSA Bulletin*. 117(1/2), 244–249. DOI: 10.1130/B25000.1.

[10] Jakeman, A.J. & Anderssen, R.S. (1975). Abel type integral equations in stereology. I. General discussion. *Journal of Microscopy.* 105, Pt. 2, 121–133.

[11] Ohser, J. & Sandau, K. (2000). Considerations About the Estimation of the Size Distribution in Wicksell's Corpuscle Problem. *Lecture Notes in Physics.* 554, 185–202.

[12] Hielbroner, R. *How to derive size distributions of particles from size distributions of sectional areas,* https://earth.unibas.ch/micro/support/PDF/grainsize.pdf

[13] Cahn, J.W. & Fullman, R.L. (1956). On the Use of Lineal Analysis for Obtaining Particle-Size Distri-bution Functions in Opaque Samples. *Trans. AIME, J. Metals.* 206, 610-12.

[14] Lord, C.W. & Willis, T.F. (1951). Calculation of air bubble distribution from results of a Rosiwal traverse of aerated concrete. *A.S.T.M. Bull.* 177, 177-187.

[15] Spektor, A.G. (1950). Analysis of distribution of spherical particles in non-transparent structures. *Zavodsk. Lab.*, 16, 173-177.

[16] Bockstiegel, G. (1966). The Porosity-Pressure Curve and its Relation to the Pore-Size Distribution in Iron Powder Compacts. in.: Modern Developments in Powder Metallurgy. H.H. Hausner (ed.), Metal Powder Industries Federation and The Metallurgical Society of AIME. pp. 155-187.

[17] Burbelko, A., Gurgul, D. & Wiktor, T. Theory of the Stereological Analysis of Spheroid Size Distribution – on a Theoretical Basis. *Archives of Foundry Engineering* (under review).

[18] Intel Math Kernel Library, Developer Reference, Revision 0.11, MKL 2017.